

Shape-induced phenomena in the finite-size antiferromagnets

Helen V. Gomonay and Vadim M. Loktev
*Bogolyubov Institute for Theoretical Physics NAS of Ukraine,
 Metrologichna str. 14-b, 03143, Kyiv, Ukraine*

It is of common knowledge that the direction of easy axis in the finite-size ferromagnetic sample is controlled by its shape. In the present paper we show that an analogous phenomenon should be observed in the compensated antiferromagnets with strong magnetoelastic coupling. Shape-induced contribution into magnetic anisotropy originates from the long-range magnetoelastic forces and can be detected by the magnetic rotational torque and AFMR measurements.

PACS numbers: 75.60.Ch, 46.25.Hf, 75.50.Ee

I. INTRODUCTION

The fact that antiferromagnetic crystals (AFM) break up into the regions with different orientation of AFM vectors below the Néel temperature was predicted theoretically by L. Néel [1] and then proved experimentally (see, e.g., [2, 3, 4, 5, 6, 7] and many others).

Domain structures observed in different AFMs have some common features that we summarize below.

1. Magnetic domains with different orientations of AFM vector are characterized by different tensors of spontaneous strain and so can be treated as deformation twins.
2. The morphology of AFM domains is similar to morphology of deformation twins in martensites. In contrast to FMs, the DS in AFMs is regular, periodic and consists of alternating stripes with different deformation.
3. Unlike FMs, domain walls (DW) are plane-like and are parallel to low-index atomic planes.
4. Deformation does not map orientation of AFM vector locally (e.g., inside the DW orientation of AFM vector is determined by competition between exchange interaction and deformation-induced anisotropy).
5. AFM domains spontaneously appear below the Néel temperature. The domain patterns observed during heating-cooling cycles through the Néel point may be either identical or similar to each other.
6. DS may be reversibly changed by external magnetic field or stress.

The properties (1)-(4) show that magnetoelastic coupling plays the leading role in formation of the DS in AFMs. It follows from (5), (6) that the DS may be considered as thermodynamically equilibrium notwithstanding the fact that the DW energy is positive and leads to an increase of free energy of the whole sample. Regularity of the DS (properties (2), (2)) excludes an entropy of domain disorder as a factor which leads to a decrease of free energy of a sample and favours formation of inhomogeneous state [8]. Properties (4)-(6) may be explained by the presence of the elastic defects (dislocations, disclinations, etc.) [9] that produce inhomogeneous stress field in the sample. This “frozen-in” *extraneous* (with respect to an ideal crystal) field stabilizes inhomogeneous distribution of AFM vector via magnetoelastic interactions and ensures reconstruction of the DS during heating/cooling cycles.

Another model [10] consistent with all the properties (1)-(6) is based on the assumption that AFM ordering is accompanied by appearance of so called quasiplastic stresses [11] coupled with the orientation of AFM vector. We assume that these *intrinsic* stresses are caused by virtual forces that represent the change of free energy of the system with displacement of an atom bearing magnetic moment. Self-consistent distribution of internal stress field depends upon the shape of the sample and is generally inhomogeneous. Equilibrium distribution of AFM vector maps the stress field and thus is also inhomogeneous and sensitive to application of external field and temperature variation.

Both the defect-based and defectless models exploiting magnetoelastic mechanism predict similar dependence of macroscopic characteristics of a sample *vs* external magnetic and stress field, but leads to different results when applied to a set of different samples. Namely, in the framework of the *defect-based* model, the domain distribution, domain size, and some other quantitative characteristics may vary depending on technological conditions and prehistory of a sample. On the contrary, the *defectless* model predicts variation of macroscopic properties for crystals of a different shape.

Below we predict shape-related phenomena in AFMs that can be experimentally tested. In the framework of the *defectless* model we calculate the effective shape-induced anisotropy which can be determined by torque measurements, and the frequency of the lowest spin-wave branch detectable by AFMR technique. We consider the case of an “easy-plane” AFM typical example of which is given by NiO, CoCl₂, or KCoF₃.

II. DESTRESSING ENERGY

According to our main assumption, the AFM vectors $\mathbf{L}(\mathbf{r})$ may be treated as quasidefects that produce intrinsic stress field $\hat{\sigma}^{(in)}(\mathbf{r})$. Thus, thermodynamic potential of the finite-size AFM can be represented as

$$\Phi[\mathbf{L}(\mathbf{r})] = \int_V \left\{ f^{\text{mag}}[\mathbf{L}(\mathbf{r})] - \frac{1}{2} \hat{\sigma}^{(in)}[\mathbf{L}(\mathbf{r})] : \hat{c}^{-1} : \hat{\sigma}^{(in)}[\mathbf{L}(\mathbf{r})] \right\} d\mathbf{r} + \Phi^{\text{dest}}. \quad (1)$$

Here f^{mag} is a “bare” magnetic energy, the second term is a self-energy of quasidefect, \hat{c}^{-1} is 4-th rank tensor of elastic stiffness, Φ^{dest} is a so-called [10] destressing energy (DE) which describes interaction between quasidefects localized at different points.

Explicit expression for DE is obtained from the requirement for mechanical equilibrium with due account of boundary conditions at the sample surface. The main nonnegative contribution arises from averaged (over the sample volume V) internal stress $\langle \hat{\sigma}^{(in)} \rangle$ and can be represented as

$$\Phi^{\text{dest}} = \frac{V}{2} \langle \hat{\sigma}_{jl}^{(in)} \rangle \hat{\aleph}_{jklm} \langle \hat{\sigma}_{km}^{(in)} \rangle, \quad \hat{\aleph}_{jklm} \equiv \frac{\partial^2}{\partial r_k \partial r_m} \int_V G_{jl}(\mathbf{r} - \mathbf{r}') d\mathbf{r}', \quad (2)$$

where $G_{km}(\mathbf{r} - \mathbf{r}')$ is a 3D Green’s function of elasticity (with zero nonsingular part) and 4-th rank symmetrical destressing tensor $\hat{\aleph}$ depends upon the sample shape.

Functional dependence between intrinsic stress tensor and AFM vector is given by a constitutive relation which should satisfy the principles of locality, material objectivity and material symmetry. The simplest form of such a relation which assumes isotropy of magnetoelastic properties of the media is

$$\sigma_{jk} = \frac{\lambda_v}{3} \mathbf{L}^2 \delta_{jk} + \lambda' \left(L_j L_k - \frac{\mathbf{L}^2}{3} \delta_{jk} \right) \quad (3)$$

where coefficients λ_v and λ' define the principal stresses of magnetoelastic nature.

Substituting (2) and (3) into (1) one comes to a closed expression for thermodynamic potential, minimization of which gives equilibrium distribution of \mathbf{L} throughout the sample.

Two terms of magnetoelastic origin in (1) have one principal distinction. The structure of the local energy contribution (second term) is defined by crystal symmetry, while the structure of Φ^{dest} depends upon the sample shape. In the framework of phenomenological approach local energy contributes to effective anisotropy constant only, while DE is responsible for the DS formation and may be a source of artificial 4th order anisotropy as will be shown below.

III. APPLICATION TO AN “EASY-PLANE” AFM

To understand the role of DE in the shape-induced phenomena we consider the simplest case of an “easy-plane” AFM (point symmetry group of the crystal includes 3-rd, 4-th or 6-th order rotations around Z -axis) cut in a form of an elliptic cylinder with a and b semiaxes (parallel to X and Y axes, respectively) and generatrix parallel to Z . The elastic properties of media are supposed to be isotropic ($c_{11} - c_{12} = 2c_{44}$). In this case nontrivial contribution to DE takes a form

$$\begin{aligned} \Phi^{\text{dest}} = & \frac{V}{2} \left\{ K_2^{\text{elas}} (L_Y^2 - L_X^2) + K_{\text{is}}^{\text{elas}} [\langle L_X^2 - L_Y^2 \rangle^2 \right. \\ & \left. + 4 \langle L_X L_Y \rangle^2] - K_{4\text{an}}^{\text{elas}} [\langle L_X^2 - L_Y^2 \rangle^2 - 4 \langle L_X L_Y \rangle^2] \right\}, \end{aligned} \quad (4)$$

where effective shape-induced anisotropy constants are

$$\begin{aligned} K_2^{\text{elas}} &= \frac{a-b}{a+b} \frac{(\lambda')^2 (2-3\nu) + \lambda_v \lambda'}{4c_{44}(1-\nu)}, \\ K_{\text{is}}^{\text{elas}} &= \frac{(\lambda')^2 (3-4\nu)}{8c_{44}(1-\nu)}, \quad K_{4\text{an}}^{\text{elas}} = \left(\frac{a-b}{a+b} \right)^2 \frac{(\lambda')^2}{6c_{44}(1-\nu)}, \end{aligned} \quad (5)$$

and $\nu = c_{12}/(c_{11} + c_{12})$ is the Poisson ratio.

Magnetic energy density of such an AFM in the external magnetic field \mathbf{H} (low compared with spin-flip value) may be written as:

$$f^{\text{mag}} = \frac{1}{2} K_2^{\text{mag}} L_Z^2 + f_{\text{in-plane}}^{\text{mag}} - \frac{1}{2} \chi [\mathbf{H} \times \mathbf{L}]^2, \quad (6)$$

Table I: Shape-induced $K_{\text{is}}^{\text{elas}}$ and magnetic $f_{\text{in-plane}}^{\text{mag}}$ anisotropy (in erg/cm³), and critical aspect ratio for typical “easy-plane” AFMs (details of calculation see in [12]).

AFM	$K_{\text{is}}^{\text{elas}}$	$f_{\text{in-plane}}^{\text{mag}}$	$(a/b)_{\text{cr}}$
NiO	$0.8 \cdot 10^4$	288	1.1
CoCl ₂	$5.6 \cdot 10^5$	$< 3 \cdot 10^4$	3.4
KCoF ₃	$3 \cdot 10^6$	$5 \cdot 10^5$	1.5

where χ is magnetic susceptibility, out-of-plane anisotropy constant $K_2^{\text{mag}} \gg K_2^{\text{elas}}$ is large enough to keep AFM vector in XY plane, and explicit form of the in-plane magnetic anisotropy $f_{\text{in-plane}}^{\text{mag}}$ is specified by a crystal symmetry.

For a typical “easy-plane” AFM $f_{\text{in-plane}}^{\text{mag}}$ is much less than the effective constants (5) of magnetoelastic nature (see table I). So, in these crystals the destressing effects may stimulate formation of DS and change equilibrium orientation of AFM vector.

It should also be stressed that three different shape-induced anisotropy constants (5) depend on the aspect ratio a/b in a different way. This opens a possibility to control macroscopic properties of the sample varying its shape.

IV. FORMATION OF THE EQUILIBRIUM DS

If in-plane magnetic anisotropy is small but not vanishing, then, the DE favours formation of DS. For example, in case of an isotropic sample ($a = b$) the only nontrivial term with $K_{\text{is}}^{\text{elas}}$ in eq. (4) is nonnegative. In the absence of external field it can only be diminished by zeroing average values of $\langle L_x^2 - L_y^2 \rangle$, $\langle L_x L_y \rangle$, i.e., by appearance of equiprobable distribution of domains with different orientation of AFM vector.

The external magnetic field causes rotation of AFM vector and removes degeneracy of various domains. Due to a long-range character of elastic forces, the field-induced ponderomotive force that acts on DW is compensated by the destressing, restoring force. Competition of these two factors determines equilibrium proportion of different domains. If, for example, external field is applied in-parallel to an “easy” direction in XY plane (say, X axis), then, the volume fraction ξ of energetically preferable Y -type domain (in which $\mathbf{L} \perp \mathbf{H}$), increases quadratically with field $\xi = 0.5[1 + (H/H_{\text{MD}})^2]$ up to monodomainization field $H_{\text{MD}} = \sqrt{K_{\text{is}}^{\text{elas}}/\chi} \propto \lambda'/\sqrt{\chi c_{44}}$.

The DS may be also observed in samples with small but nonzero eccentricity ($a \approx b$) providing that in-plane magnetic anisotropy is large enough to keep two different equilibrium (stable and metastable) \mathbf{L} orientations: $K_2^{\text{elas}} \leq f_{\text{in-plane}}^{\text{mag}}$. In this case it is the shape factor that removes degeneracy and hence equiprobability of the domains. In the above example the fraction of X -type domain ($\mathbf{L} \parallel X$) depends on the aspect ratio as follows

$$\xi - \frac{1}{2} = \frac{K_2^{\text{elas}}}{K_{4\text{an}}^{\text{elas}}} \propto \frac{b-a}{b+a} \quad (7)$$

and the DS reproduces the orthorhombic symmetry of the sample.

Critical values of aspect ratio $(a/b)_{\text{cr}}$ (obtained from the condition $K_2^{\text{elas}} = f_{\text{in-plane}}^{\text{mag}}$) at which equilibrium DS is still thermodynamically favourable are given in the last column of table I.

V. TORQUE EFFECT

If the aspect ratio a/b of the sample noticeably differs from 1, then, all the effective anisotropy constants in (4) have the same order of value and are much greater than in-plane anisotropy, $K_{\text{is}}^{\text{elas}} \gg f_{\text{in-plane}}^{\text{mag}}$ (see table I). So, the sample has shape-induced uniaxial anisotropy regardless of its crystallographic symmetry.

An appropriate tool for measuring anisotropy constants is a rotational torque of untwinned crystal in the magnetic field. If the rotational axis is perpendicular to “easy-plane” XY and magnetic field makes a ψ angle with X axis (see inset in fig. 1), then the rotational torque can be calculated as $-\partial\Phi/\partial\psi$ where free energy potential Φ is given by eq. (1). With account of the eqs. (4)-(6) the rotational torque per unit volume is represented as

$$T(\psi) = K_2^{\text{elas}} \sin 2\theta(\psi) + 2K_{4\text{an}}^{\text{elas}} \sin 4\theta(\psi), \quad (8)$$

where a θ angle between AFM vector and X axis unambiguously determines equilibrium orientation of \mathbf{L} and is calculated from the condition for minimum of the potential (1):

$$K_2^{\text{elas}} \sin 2\theta + 2K_{4\text{an}}^{\text{elas}} \sin 4\theta - \frac{1}{2}\chi H^2 \sin 2(\theta - \psi) = 0. \quad (9)$$

Analysis of eqs. (8)-(9) shows that i) effective anisotropy is determined by shape-dependent (via a/b ratio) constants

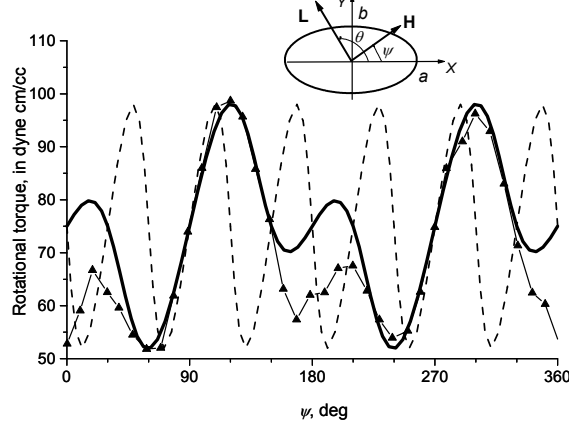


Figure 1: Rotational torque of untwinned NiO crystal at RT in $H=4.8$ kOe for [111] rotational axis. Triangles - experimental data [13], solid line - theoretical approximation according to (8), (9), dashed line - approximation of infinite crystal (no shape effect).

$K_2^{\text{elas}}, K_{4\text{an}}^{\text{elas}}$; ii) shape-induced anisotropy removes multiaxial degeneracy of equilibrium orientation of AFM vector and thus excludes formation of DS; iii) in absence of the field preferred orientation of AFM vector coincides with the longer ellipse axis ($K_2^{\text{elas}} > 0, a > b$); iv) external magnetic field applied along the longer ellipse axis may induce spin-flop transition at $H = H_{\text{SF}}$, where spin-flop field

$$H_{\text{SF}} = \sqrt{\frac{1}{\chi} |K_2^{\text{elas}} - 4K_{4\text{an}}^{\text{elas}}|} \propto \frac{\lambda'}{\sqrt{\chi c_{44}}} \sqrt{\frac{a-b}{a+b}} \quad (10)$$

is governed by the sample shape and is independent of crystalline anisotropy.

An interesting result is obtained for the sample having a square cross-section. In this case equilibrium distribution of AFM vector is inhomogeneous in principle but in average can still be described by eq. (9) with

$$K_2^{\text{elas}} = 0, \quad K_{4\text{an}}^{\text{elas}} = \frac{\ln 2(\lambda')^2}{\pi c_{44}(1-\nu)} > 0. \quad (11)$$

It is obvious that such a sample shows 4-th order effective anisotropy with “easy axes” directed along square diagonal (45° angle with respect to X axis, as results from condition $K_{4\text{an}}^{\text{elas}} > 0$).

The rotational torque calculated from eqs. (8), (9) for a typical AFM NiO is shown in figs. 1, 2. In calculations we use experimental results [13] for a rotational torque around [111] axis taken at room temperature for $H=4.8$ kOe (triangles in fig. 1). Since the experiment shows strong hysteresis in clock-wise and counter-clock wise rotations, the data in fig. 1 are preliminarily averaged over cc-ccw cycle. Theoretical curve (solid line) includes some nonzero average torque that may result from inhomogeneity of the sample, and adjusting parameters are $\chi = 4.35 \cdot 10^{-4}$ emu/cm³, $K_2^{\text{elas}} = 900$ erg/cm³, $K_{4\text{an}}^{\text{elas}} = 450$ erg/cm³, $a/b = 20$.

Four curves in fig. 2 demonstrate possible variation of the rotational torque with the crystal shape. For a large aspect ratio (curve (a)) contributions from both 2-nd and 4-th order anisotropy terms are equally important ($K_2^{\text{elas}} \propto K_{4\text{an}}^{\text{elas}}$), the torque curve is composed of $\sin 2\theta$ and $\sin 4\theta$ components. At lower aspect ratio (curves (b), (c)) the 4-th order component becomes less pronounced and the amplitude of torque also diminishes. A circular cylinder ($a = b$) will show no shape effect in a single domain state, but a sample with a square cross-section should posses 4-th order anisotropy (as seen from curve (d)) regardless of crystalline symmetry.

Evidently, shape-dependence of the magnetic rotational torque for NiO crystal was observed in Ref. [13]. The authors notice that “a nearly pure $\sin 4\theta$ curve is obtained when the (111) cross section is square”. For an arbitrary shaped section the experimental curve (fig. 1, triangles) is satisfactorily fitted with combination of $\sin 2\theta$ and $\sin 4\theta$

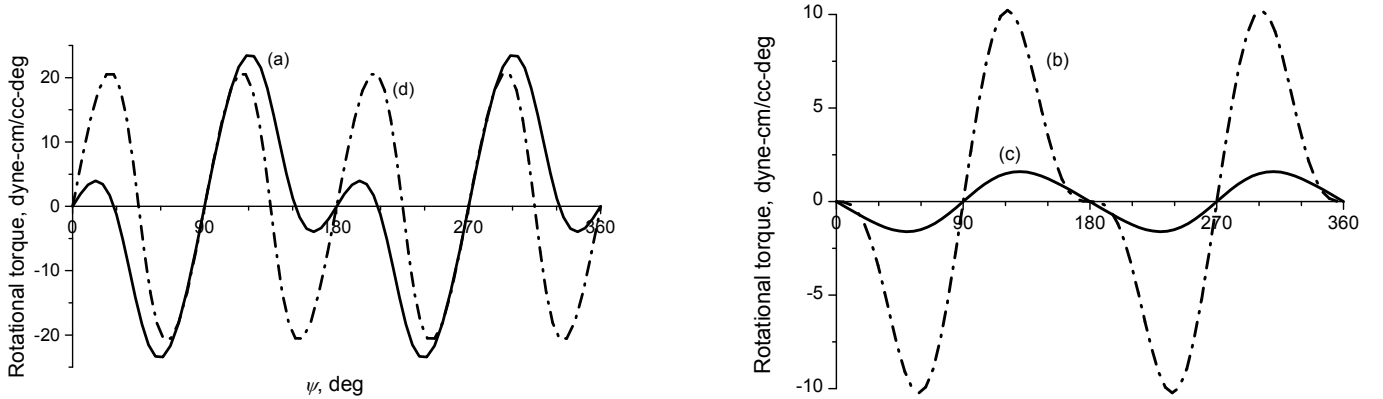


Figure 2: Rotational torque (calculated) of untwinned NiO crystal at RT in $H=5$ kOe for [111] rotational axis for the samples with different shape. For ellipse-section samples an aspect ratio is $a/b = 20$ (a); 3 (b); 1.2 (c); (d) – square-section sample.

components (solid line). Dashed line in fig. 1 shows theoretical curve with $f_{\text{in-plane}}^{\text{mag}} = 220 \cos 6\theta$ erg/cm³ that could be expected in neglection of shape-induced effects. The presence of $\sin 4\theta$ component in the rotational torque makes it possible to exclude the effect of \mathbf{L} “freezing” by magnetoelastic strain which may be expected in relatively small magnetic field. Additional anisotropy induced by frozen lattice is uniaxial and should be insensible to the variation of a crystal shape.

VI. AFMR

The effect of shape-induced anisotropy may also be detected by measuring frequency of the lowest branch of a spin-wave spectrum. AFMR frequency calculated within a standard Lagrangian technique in long-wave approximation is given by the expression

$$\nu_{\text{AFMR}} = g \sqrt{\frac{2}{\chi} (K_{\text{is}}^{\text{elas}} + K_2^{\text{elas}} \cos 2\theta + 4K_{4\text{an}}^{\text{elas}} \cos 4\theta - \chi H^2 \cos 2(\theta - \psi))}, \quad (12)$$

where g is gyromagnetic ratio and equilibrium value of θ may be calculated from (9). Polar diagram of $\nu_{\text{AFMR}}(\psi)$ calculated from (12) for NiO ($g = 2, 5$) for a different crystal shape is shown in fig. 3. For the aspect ratio close to 1 (dotted line) the shape effect is negligible and magnetoelastic gap in AFMR spectrum is almost isotropic. For elongated (dash-dotted and dashed lines) or square-shaped (solid line) samples the AFMR gap should show strong 2-fold or 4-fold anisotropy.

VII. CONCLUSIONS

In summary, we propose a model that describes AFM with the pronounced magnetoelastic coupling. The model is based on the assumption that AFM ordering is accompanied by appearance of elastic dipoles. Due to the long-range nature of elastic forces, in the finite-size sample the energy of dipole-dipole interaction (destressing energy) depends on the crystal shape and is proportional to its volume.

The model predicts existence of shape-induced magnetic anisotropy which corresponds to macroscopic symmetry of the sample and can be detected by the magnetic rotational torque and AFMR measurements.

[1] Néel L., Proc. International Conf. Theor. Physics. Kyoto and Tokyo. Science Council of Japan, Tokyo. 701 (1953).
[2] Wilkinson M. K., Cable J. W., Wollan E. O. and Koehler W. C., Phys. Rev **113**, 497 (1959).
[3] Tanner B. K., Safa M., Midgley D. and Bordas J., JMMM **1**, 337 (1976).
[4] Baruchel J., Schlenker M. and Roth W. L., J. Appl. Phys **48**, 5 (1977).
[5] Janossy A., Simon F., Feher T., Rockenbauer A., Korecz L., Chen C., Chowdhury A. J. S. and Hodby J.W., Phys. Rev. B **59**, 1176 (1999).

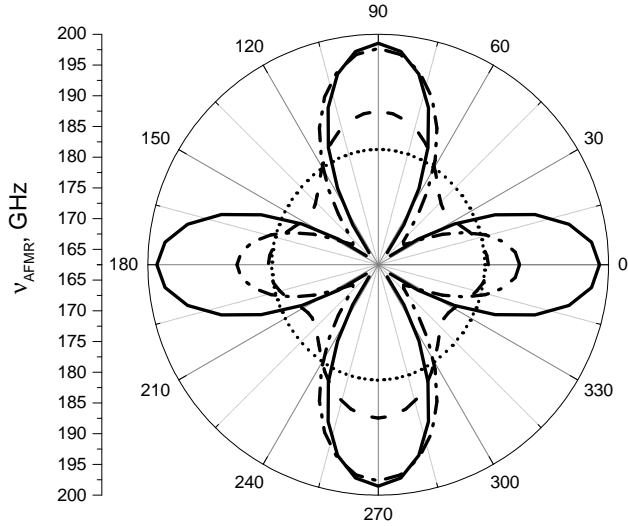


Figure 3: Angular dependence of AFMR frequency vs magnetic field orientation for samples with different aspect ratio: $a/b = 20$ (dash-dotted line); 3 (dashed line); 1.2 (dotted line). Solid line corresponds to a square-section sample.

- [6] Scholl A., Stöhr J., Lüning J., Seo J. W., Fompeyrine J., Siegwart H., Locquet J. P., Nolting F., Anders S., Fullerton E. E., Schneifein M. R. and Padmore H. A., *Science* **287**, 1014 (2000).
- [7] Weber N. B., Bethke C. and Hillebrecht F. U., *JMMM* **226**, 1573 (2001).
- [8] Li Y. Y., *Phys. Rev* **101**, 1450 (1956).
- [9] Kalita V. M., Losenko A. F., Ryabchenko S. M., Trotsenko P. A. and Yatkevich T. M., *Fizika tverdogo tela* **46**, 317 (2004).
- [10] Gomonay H. V. and Loktev V. M., *Physics of the Solid State* **47**, 1755 (2005).
- [11] Kléman M. and Schlenker M., *J. Appl. Phys.* **43**, 3184 (1972).
- [12] Gomonay H. V. and Loktev V. M., *J. Physics: Cond. Matter* **14**, 3959 (2002).
- [13] Roth W. L. and Slack G. A., *J. Appl. Phys* **31**, S352 (1960).